C_s **Template (*Z,Z*)-Deca-4,8-diene-1,10-dicarboxylate 28.** By use of general procedure B, template C_s diol 10 (200 mg, 0.29 mmol) and (*Z,Z*)-deca-4,8-diene-1,10-dicarboxylic acid (30) (65 mg, 0.29 mmol) were combined to furnish 103 mg of bislactone 28 (40%) following flash chromatography on silica gel with CH_2Cl_2 as eluent: IR (CCl_4) 1743 cm⁻¹ (C=O); ¹H NMR (200 MHz, $CDCl_3$) δ 7.27–7.05 (m, 16 H, Ar H), 5.48–5.30 (m, 6 H, C*H*=CH, C(*H*)HO), 5.00 (d, *J* = 11.5 Hz, 2 H, C(H)*H*O), 4.17 (s, 2 H, bridgehead H), 2.48–2.36 (m, 4 H, C*H₂*CO₂), 2.10–1.06 (m, 30 H), –0.37 (d, *J* = 11.3 Hz, 2 H, H over Ar); ¹³C NMR (75 MHz, $CDCl_3$) δ 173.3, 145.3, 143.8, 142.6, 141.2, 130.4, 127.6, 126.1, 125.9, 125.5, 125.3, 124.3, 123.1, 121.5, 121.0, 62.6, 48.4, 48.3, 47.6, 47.4, 47.2, 46.9, 42.6, 41.9, 41.7, 41.6, 41.5, 39.3, 34.6, 28.8, 28.3, 27.1, 23.6; FABMS *m/z* (relative intensity) 882 (70, M⁺).

C_2 **Template Docosanedioate 26a.** By use of general procedure B, template C_2 diol 11 (100 mg, 0.14 mmol) and docosanedioic acid (53 mg, 0.14 mmol) were coupled to deliver 21 mg of bislactone 26a (14%) following flash chromatography on silica gel with CH_2Cl_2 as eluent: IR (CCl_4) 1740 cm⁻¹ (C=O); ¹H NMR (360 MHz, $CDCl_3$) δ 7.21–7.03 (m, 16 H, Ar H), 5.25 (d, *J* = 11.3 Hz, 2 H, C(*H*)HO), 5.11 (d, *J* = 11.3 Hz, 2 H, C(H)*H*O), 4.16 (s, 2 H, bridgehead H), 2.43–2.39 (m, 4 H, C*H₂*CO₂), 1.79–1.09 (m, 58 H), –0.40 (d, *J* = 10.6 Hz, 2 H, H over Ar); ¹³C NMR (75 MHz, $CDCl_3$) δ 173.9, 145.3, 143.8, 142.9, 141.4, 126.0, 125.9, 125.5, 125.3, 124.3, 123.1, 121.7, 121.0, 62.8, 48.5, 48.2, 47.2, 47.0, 42.8, 42.3, 42.2, 41.3, 39.5, 34.8, 29.7, 29.4, 29.2, 29.0, 28.9, 28.8, 28.7, 28.2,

25.1; FABMS *m/z* (relative intensity) 1027 (97, M⁺ + H).

C_2 **Template Tetracosanedioate 26b.** By use of general procedure A, template C_2 diol 11 (69 mg, 0.10 mmol), (dimethylamino)pyridine (28 mg, 0.23 mmol), and tetracosanedioyl chloride (44 mg, 0.10 mmol) were combined to yield 9 mg of bislactone 26b (9%) following flash chromatography on silica gel with 1:1 hexane/dichloromethane as eluent: IR (CCl_4) 1736 cm⁻¹ (C=O); ¹H NMR (300 MHz, $CDCl_3$) δ 7.26–7.03 (m, 16 H, Ar H), 5.2 (d, *J* = 11.5 Hz, 2 H, C(*H*)HO), 5.12 (d, *J* = 11.5 Hz, 2 H, C(H)*H*O), 4.17 (s, 2 H, bridgehead H), 2.41 (t, *J* = 7.2 Hz, 4 H, C*H₂*CO₂), 1.79–1.09 (m, 62 H), –0.41 (d, *J* = 11.1 Hz, 2 H, H over Ar); ¹³C NMR (50 MHz $CDCl_3$) δ 173.9, 145.3, 143.7, 142.8, 141.3, 126.0, 125.9, 125.8, 125.3, 124.3, 123.1, 121.6, 121.2, 48.6, 48.3, 47.4, 47.3, 47.26, 47.2, 42.8, 42.3, 42.2, 41.4, 39.6, 34.7, 34.5, 29.5, 29.4, 28.38, 28.7, 25.3, 20.7; FABMS *m/z* (relative intensity) 1055 (64, M⁺ + H).

Supplementary Material Available: Copies of ¹³C NMR spectra for 8, 9, 11, 13, 17, 1, 20, 23a, 26a, and 27 and experimental details/spectroscopic characterization for 11, 12b, 15, 16, 18, 19, 29, and 30 (18 pages). Ordering information is given on any current masthead page.

Transition Structures for the Aldol Reactions of Anionic, Lithium, and Boron Enolates

Yi Li, Michael N. Paddon-Row,[1] and K. N. Houk*

Department of Chemistry and Biochemistry, University of California, Los Angeles, Los Angeles, California 90024-1569

Transition structures for the reactions of acetaldehyde enolate and lithium and boron enolates of acetaldehyde with formaldehyde have been located with ab initio molecular orbital calculations. For the reaction of acetaldehyde enolate with formaldehyde, three transition structures were located. The transition structure for the reaction of lithium enolate with formaldehyde has a half-chair conformation, with the lithium, oxygens, and adjacent carbons in a plane. Both chair and twist-boat transition structures have been located for the reaction of boron acetaldehyde enolate with formaldehyde. The chair is 1.4 kcal/mol higher in energy than the twist-boat for the parent reaction, while methyl substituents at various positions alter these relative conformational energies. The preference for chair transition structures is large for *Z*-enolates, while twist-boat transition structures are only slightly less stable than the chair for reactions of *E*-enolates.

Introduction

Aldol reactions of metal enolates with carbonyl compounds in solution are among the most useful methods of carbon–carbon bond formation.[2,3] As shown in eq 1, the reactions of metal enolates with aldehydes can give either syn or anti aldols. The formation of a CC bond to give products with desirable functionality, frequently with stereocontrol, has made this reaction an extremely useful process.

(*Z*): R_Z = alkyl, R_E = H
(*E*): R_E = alkyl, R_Z = H
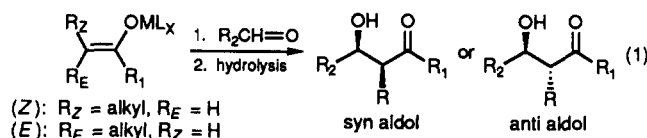
The stereochemistries of reactions of substituted enolates with aldehydes have led to qualitative inferences about transition state geometries.[3–15] As described below,

(1) Permanent address: The University of New South Wales, New South Wales, Australia.

(2) (a) Heathcock, C. H. *Science* 1981, *214*, 395. (b) Masamune, S. In *Organic Synthesis, Today and Tomorrow*; Trost, B. M., Hutchison, R., Eds., Pergamon Press: New York, 1981; p 197. (c) Mukaiyama, T. *Org. React.* 1982, *28*, 203. (d) Braun, M. *Angew. Chem., Int. Ed. Engl.* 1987, *26*, 24.

(3) (a) Heathcock, C. H. In *Asymmetric Synthesis*; Morrison, J. D., Ed.; Academic Press: New York, 1983; Vol. 3, Chapter 2, see especially pp 154–161 for an excellent summary of hypotheses about transition state geometries. (b) Evans, D. A.; Nelson, J. V.; Taber, T. R. In *Topics in Stereochemistry*; Wiley-Interscience: New York, 1982; Vol. 13, p 1.

(4) Zimmerman, H. E.; Traxler, M. D. *J. Am. Chem. Soc.* 1957, *79*, 1920.

(5) (a) Heathcock, C. H.; Buse, C. T.; Kleschick, W. A.; Pirrung, M. C.; Sohn, J. E.; Lampe, J. *J. Org. Chem.* 1980, *45*, 1066. (b) Evans, D. A.; Vogel, E.; Nelson, J. V. *J. Am. Chem. Soc.* 1979, *101*, 6120. Evans, D. A.; Nelson, J. V.; Vogel, E.; Taber, T. R. *J. Am. Chem. Soc.* 1981, *103*, 3099.
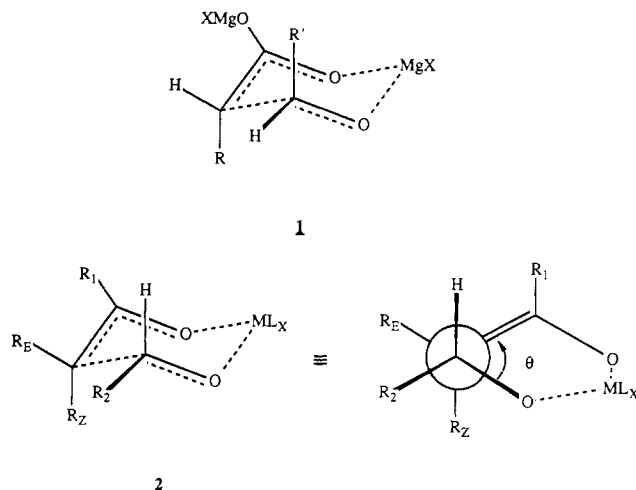
Figure 1. The Zimmerman–Traxler model (1) and the "pericyclic" chair transition state model (2) for aldol reactions.

Table I. Stereoselective Aldol Reactions of Ketone Enolates with Benzaldehyde [Eq 1, Where R_2 = Ph, R_Z = R_E = methyl]

ML_X^+	R_1 = Ph $Z:E$ → syn:anti	R_1 = Et $Z:E$ → syn:anti	R_1 = t-Bu $Z:E$ → syn:anti
Li^+	98:2 → 88:1	66:34 → 77:23	98:2 → 98:2
		30:70 → 64:36	
$B(^nBu)_2^+$	99:1 → 97:3	97:3 → 97:3	99:1 → 97:3
		69:31 → 72:28	
TAS^+	100:0 → 95:5	100:0 → 86:14	
	0:100 → 94:6	0:100 → 63:37	
$Ti(O^iPr)_2^+$	98:2 → 87:13	92:8 → 88:12	98:2 → 87:13
		36:64 → 89:11	

an amazing number of transition states and an impressive variety of effects have been invoked to rationalize these results. In order to bring theory to bear on this problem, we have undertaken a theoretical study of aldol reactions, and report here our first steps in what promises to be a long and complex journey to understand these reactions completely.[16]

We have located the ab initio RHF 3-21G transition structures for the gas-phase aldol reactions of acetaldehyde enolate with formaldehyde and for the reactions of lithium and boron acetaldehyde enolates with formaldehyde. We have also located transition structures for the reaction of boron acetaldehyde enolate with acetaldehyde and for the reactions of E- and Z-enolates of propionaldehyde with formaldehyde. While these results are only strictly relevant to the gas phase, and do not include the doubtless powerful influence of solvation, they do reveal geometrical and conformational features inherent to the isolated reactants. These features will be helpful in interpreting the influence of counterions and solvation, which are under

investigation in our laboratories and elsewhere.

The transition structures reported here for the free enolate reactions are also examples of nucleophilic additions to carbonyl groups occurring through acyclic transition structures. These results provide theoretical information of the angle of attack of nucleophiles on carbonyls in acyclic transition structures. Most previous calculated nucleophilic addition transition structures involved cyclic transition states (H_2O,[17] NH_3,[18] BH_4^-,[19] organometallics[20]). Information about trajectories of attack have also been obtained from X-ray crystallographic studies of model compounds which mimic the transition states for nucleophilic additions.[21] Model transition structure calculations have also been performed,[22] but since simple unstabilized charged nucleophiles add to carbonyls with small or nonexistent barriers in the gas phase, there have been few authentic transition structures for nucleophilic additions.[23-25] Qualitative theoretical descriptions of factors influencing nucleophilic attack trajectories have also been published.[26,27]

Empirical Models for Aldol Transition Structures.
Zimmerman and Traxler first proposed what is now called a "pericyclic" chairlike six-membered ring transition state model (1) to rationalize the stereochemistry of the Ivanov reaction.[4] Alkyl substituents of the carboxylic acid dianion and the aldehyde moiety occupy the axial positions in the preferred conformation of the original Zimmerman–

(6) (a) Dubois, J. E.; Fellmann, P. *Tetrahedron Lett.* 1975, 1225. (b) Fellmann, P.; Dubois, J. E. *Tetrahedron* 1978, *34*, 1349.

(7) Evans, D. A.; McGee, L. R. *Tetrahedron Lett.* 1980, 3975.

(8) (a) Noyori, R.; Nishida, I.; Sakata, J. *J. Am. Chem. Soc.* 1983, *105*, 1598; 1981, *103*, 2106. (b) For MM2 analysis on the steric interactions in acyclic aldol transition states see: Dougherty, D. *Tetrahedron Lett.* 1982, 4891.

(9) (a) Mulzer, J.; Zippel, M.; Brüntrup, G.; Segner, J.; Finke, J. *Justus Liebigs Ann. Chem.* 1980, 1108. (b) Mulzer, J.; Brüntrup, G.; Finke, J.; Zippel, M. *J. Am. Chem. Soc.* 1979, *101*, 7723.

(10) (a) Tin: Harada, T.; Mukaiyama, T. *Chem. Lett.* 1982, 467. Yamamoto, Y.; Yatagai, H.; Maruyama, K. *J. Chem. Soc., Chem. Commun.* 1981, 162. Nakamura, E.; Kuwajima, I. *Tetrahedron Lett.* 1983, 3347. (b) Zirconium: Yamamoto, Y.; Maruyama, K. *Tetrahedron Lett.* 1980, 4607. (c) Titanium: Nakamura, E.; Kuwajima, I. *Tetrahedron Lett.* 1983, 3343. Nakamura, E.; Kuwajima, I. *Acc. Chem. Res.* 1985, *18*, 181 and references cited therein. Reetz, M. T.; Peter, R. *Tetrahedron Lett.* 1981, 4691.

(11) (a) Gennari, C.; Colombo, L.; Scolastico, C.; Todeschini, R. *Tetrahedron* 1984, *40*, 4051. (b) Gennari, C.; Bernardi, A.; Cardani, S.; Scolastico, C. *Tetrahedron* 1984, *40*, 4059. (c) Gennari, C.; Cardani, S.; Colombo, L.; Scolastico, C. *Tetrahedron Lett.* 1984, 2283. (d) Hoffmann, R. W.; Ditrich, K. *Tetrahedron Lett.* 1984, 1781.

(12) Hoffmann, R. W.; Ditrich, K.; Froech, S.; Cremer, D. *Tetrahedron* 1985, *41*, 5517.

(13) Gennari, C.; Todeschini, R.; Beretta, M. G.; Favini, G.; Scolastico, C. *J. Org. Chem.* 1986, *51*, 612.

(14) Seebach, D.; Golinski, J. *Helv. Chim. Acta* 1981, *64*, 1413. See also: Brook, M. A.; Seebach, D. *Can. J. Chem.* 1987, *65*, 836 and references cited therein.

(15) Anh, N. T.; Thanh, B. T. *Nouv. J. Chim.* 1986, *10*, 681.

(16) (a) Preliminary results were reported as a communication: Li, Y.; Paddon-Row, M. N.; Houk, K. N. *J. Am. Chem. Soc.* 1988, *110*, 3684. (b) The potential surfaces for lithium enolate plus formaldehyde and lithium enolate plus ketene have been computed: Leung-Tong, R.; Tidwell, T. T., submitted for publication.

(17) Williams, I. H.; Spangler, D.; Maggiora, G. M.; Schowen, R. L. *J. Am. Chem. Soc.* 1985, *107*, 7717.

(18) Yamataka, H.; Nagase, S.; Ando, T.; Hanafusa, T. *J. Am. Chem. Soc.* 1986, *108*, 601.

(19) Eisenstein, O.; Schlegel, H. B.; Kayser, M. M. *J. Org. Chem.* 1982, *47*, 2886.

(20) (a) Wu, Y.-D.; Houk, K. N. *J. Am. Chem. Soc.* 1987, *109*, 908. (b) Nagase, S.; Uchibori, Y. *Tetrahedron Lett.* 1982, 2585. (c) Kaufman, E.; Schleyer, P. v. R.; Houk, K. N.; Wu, Y.-D. *J. Am. Chem. Soc.* 1985, *107*, 5560. (d) Bachrach, S. M.; Streitwieser, A., Jr. *J. Am. Chem. Soc.* 1986, *108*, 3946.

(21) (a) Bürgi, H. B.; Dunitz, J. D.; Shefter, E. *J. Am. Chem. Soc.* 1973, *95*, 5065. (b) Dunitz, J. D. *X-Ray Analysis and the Structures of Organic Molecules*; Cornell University Press: Ithaca, NY, 1979; pp 366–384 and references therein. (c) Bürgi, H. B.; Shefter, E.; Dunitz, J. D. *Tetrahedron* 1975, *31*, 3089.

(22) (a) Bürgi, H. B.; Lehn, J. M.; Eipff, G. *J. Am. Chem. Soc.* 1974, *96*, 1956. (b) Bürgi, H. B.; Dunitz, J. D.; Lehn, J. M.; Wipff, G. *Tetrahedron* 1974, *30*, 1563. (c) Scheiner, S.; Lipscomb, W. N.; Kleier, D. A. *J. Am. Chem. Soc.* 1976, *98*, 4770. (d) Anh, N. T.; Eisenstein, O. *Nouv. J. Chem.* 1977, *1*, 61.

(23) (a) Bernardi, F.; Olivucci, M.; Poggi, G.; Robb, M. A.; Tonachini, G. *Chem. Phys. Lett.* 1988, *144*, 141. (b) Bayly, C. I.; Grein, F. *Can. J. Chem.* 1988, *66*, 149.

(24) (a) Wu, Y.-D.; Houk, K. N. *J. Am. Chem. Soc.* 1987, *109*, 906. (b) Ewig, C. L.; Wazer, J. R. V. *J. Am. Chem. Soc.* 1986, *108*, 4774.

(25) Madura, J. D.; Jorgenson, W. L. *J. Am. Chem. Soc.* 1986, *108*, 2517.

(26) Houk, K. N.; Paddon-Row, M. N.; Rondan, N. G.; Wu, Y.-D.; Brown, F. K.; Spellmeyer, D. C.; Metz, J. T.; Li, Y.; Loncharich, R. J. *Science* 1986, *231*, 1109.

(27) (a) Liotta, C. L.; Burgess, E. M.; Eberhardt, W. H. *J. Am. Chem. Soc.* 1984, *106*, 4849. (b) Stone, A. J.; Erskine, R. W. *J. Am. Chem. Soc.* 1980, *102*, 7185. (c) Lodge, E. P.; Heathcock, C. H. *J. Am. Chem. Soc.* 1987, *109*, 3353. (d) Mori, I.; Bartlett, P. A.; Heathcock, C. H. *J. Am. Chem. Soc.* 1987, *109*, 7199.
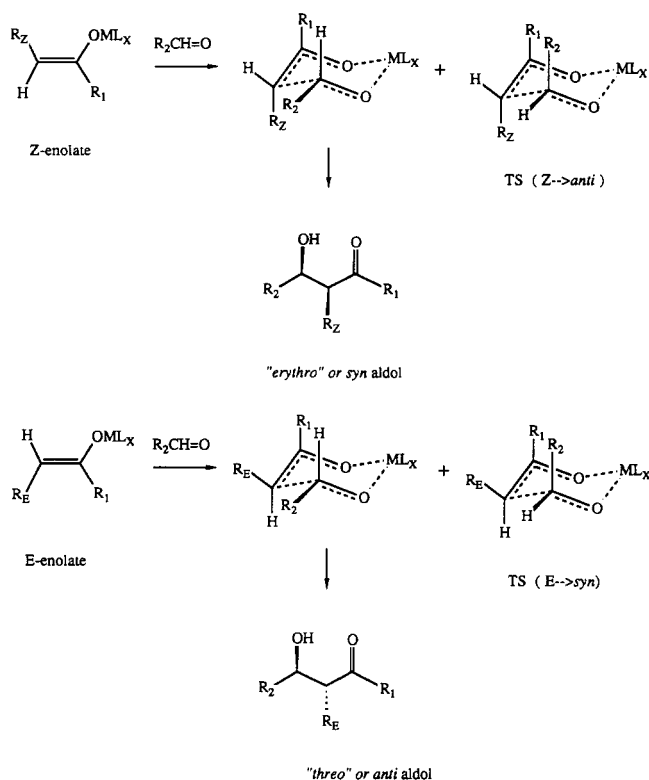
Figure 2. "Pericyclic" chair transition state models for formation of the major products of aldol reactions of *Z*- and *E*-enolates.

Figure 3. Skewed transition-state models for aldol reactions of *Z*- and *E*-enolates.

Traxler transition state. The chairlike model, but not the axial conformation for alkyl groups, was adopted by many from the Zimmerman–Traxler transition state model, and has been accepted generally for the rationalization of stereochemistry of the aldol reaction.[3] This model (2) for the aldol reaction transition state is shown in two views in Figure 1. The side view shows the resemblance of the transition state to a chair cyclohexane, while the Newman projection along the forming CC bond shows more intimately the relationship between the various substituents on the aldehyde and on the enolate terminus. The chair transition state is staggered about the forming CC bond. The metal, M^+, is most frequently Li^+, and L_X represents one or more ligands, or associated solvent. In some cases the lithium reagents are aggregated. Many other metal cations have been studied, with Al^{3+}, Zn^{2+}, Mg^{2+}, R_2B^+ (covalently bound to oxygen) or a variety of other counterions giving qualitatively similar results.[3] The metal cation chelates the oxygens and thus enforces a more or less gauche arrangement of the vicinal C=O and C=C bonds. Table I shows some exemplary data on stereoselectivities for reactions of various types of metal enolates with aldehydes.[5] Such data have been used to make the following deductions about the transition states of aldol reactions.

For either *Z*-enolates (R_Z = alkyl or aryl, R_E = H) or *E*-enolates (R_E = alkyl or aryl, R_Z = H) with strongly coordinating cations such as Li^+, low stereoselectivity is observed when R_1 is a small group. When R_1 is large, relatively high stereoselectivity is found; *Z*-enolates react to form preferentially "erythro", or syn, products (as shown in Figure 2), and *E*-enolates lead to "threo", or anti, products.[3] In the models shown in Figures 1 and 2, the favored product can be seen to arise from the transition structure which has the aldehyde substituent, R_2, in a quasi-equatorial, rather than quasi-axial conformation. The model satisfactorily rationalizes the increase in stereoselectivity caused by an increase in the size of R_1, since
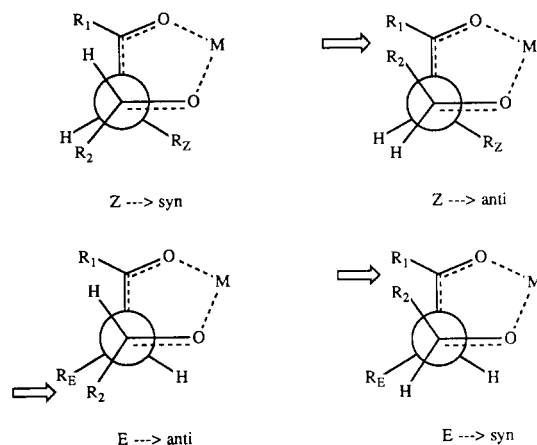
a larger R_1 should destabilize a conformation with an axial R_2 group.

Z-Enolates react with higher stereoselectivity than the corresponding *E*-enolates.[3,6] This trend is not readily explained by the perfectly staggered models shown in Figure 2. Both transition states minimize the interaction between R_1 and R_2, but the preferred *Z*-enolate transition structure should also have a destabilizing interaction between R_2 and R_Z which could be relieved in the *Z* → anti transition structure. In the transition structures involving the *E*-enolate, both syn and anti transition structures have similar gauche R_2–R_E interactions, so it might be expected that stereoselectivity would be high, and dominated by the tendency to minimize the R_1–R_2 interaction. However, the *E*-enolates react with lower stereoselectivity than corresponding *Z*-enolates.

In order to account for these phenomena, it has been suggested by Dubois, Healthcock, and others,[3a,6] that the transition state could have a C=C—C=O torsional angle closer to 90°. As shown in Figure 3, the preferred *Z* → syn transition structure will now have R_2 far from both R_1 and R_Z groups, while the *Z* → anti transition structure places R_2 quite near R_1. The partial eclipsing of R_2 with H in the transition structure leading to syn is presumed to be of minor importance. For the *E*-enolate, R_2 and R_E interfere in the *E* → anti transition structure, while R_1 and R_2 are in close proximity in the *E* → syn transition structure. The anti product is favored when R_1 is large, but not by a large amount. These 90° transition states may arise in order to accommodate the 1.9–2.1 Å metal–oxygen distances expected for Li^+, Mg^{2+}, and Zn^{2+} enolates among others.[3]

This 90° model also provides an explanation for the fact that reverse stereoselectivities are observed for very large R_E and R_Z groups (e.g., *t*-Bu). In such a case, the *Z* → anti and *E* → syn 90° transition structures place the R_2 far from the very large R_Z or R_E groups.

Evans has proposed an alternative explanation for the change of stereoselectivity as the R_E and R_Z groups become bulky. He proposed that boat transition states as shown in Figure 4 might also be significant. These "0°" conformations are suggested to be preferred when R_Z or R_E are very large.[3b,7] Evans' model predicts that an increase of R_Z size would give more anti product, because the boat becomes an alternative to the chair. On the other hand, an increase of the size of R_E would have little effect on the stereoselectivity.

Aldol reactions involving nonchelating cations (e.g., M^+ = TAS^+ = $(Et_2N)_3S^+$)[8] presumably involve the "open", or "180°", transition state (Figure 5) and give the "erythro" (syn) product from either *Z*- or *E*-enolates.[8] Such open
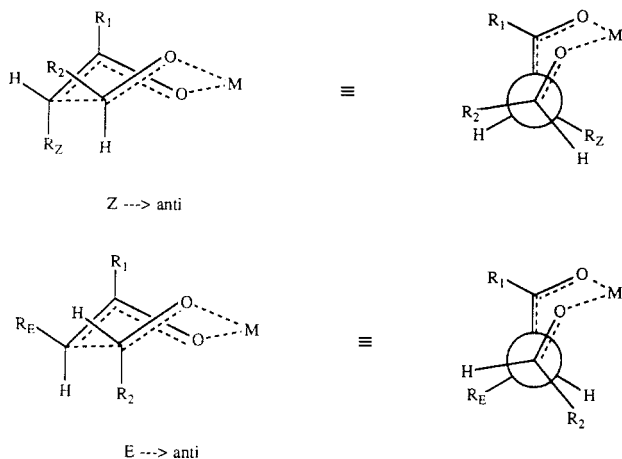
Figure 4. Evans boat transition state models for aldol reactions of *Z*- and *E*-enolates, where R_Z and R_E are large.
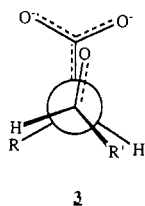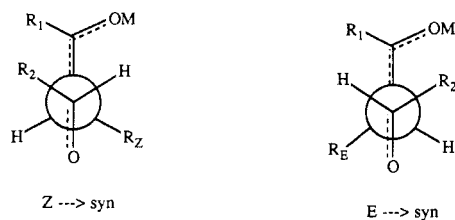

Figure 5. "Open" acyclic transition state models for aldol reaction with nonchelating cations. At the bottom, the Mulzer model (3) for the formation of the anti product from carboxylic acid dianions is shown.
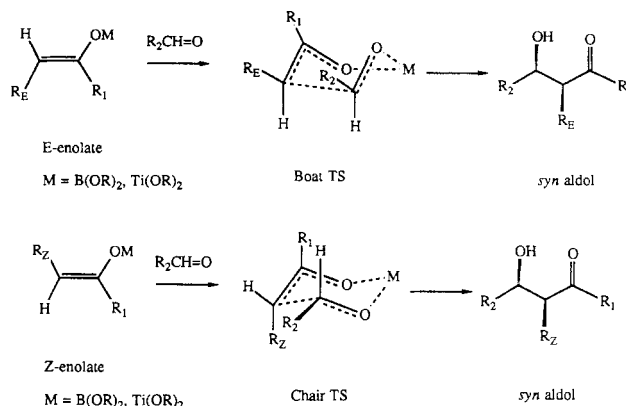

Figure 6. The preferred twist-boat transition state for the aldol reactions of *E*-enol borates and the preferred chair transition state for the aldol reactions of *Z*-enol borates.
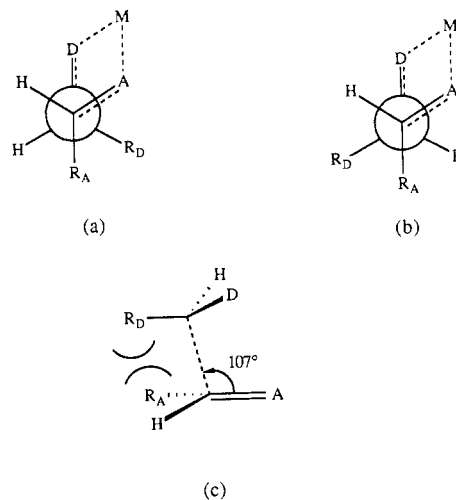

Figure 7. The Seebach–Golinski transition states for aldol reactions and related additions of unsaturated donors to unsaturated acceptors. The drawing at the bottom (c) shows one possible origin of the preference for (a) over (b).

transition state models are often invoked whenever both *Z*- and *E*-enolates give the same product. In this model, the stereochemistry of the product is determined by the minimization of repulsion between R_2 and R_Z or R_E.

Mulzer found that the reaction of carboxylic acid dianions with aldehydes always gives the anti product.[9] He proposed that the 0° transition state (3) was favored for such reactions, and anti products were formed to minimize repulsion between R's. Addition of cation coordinators increases the anti preference. Attractive secondary orbital interactions between orbitals on oxygens in the dianion HOMO and aldehyde LUMO were proposed to account for this unusual preference.[9]

Some other metals (e.g. Sn, Zr, Ti, B(OR)₂) give the same *syn* product from the *Z*- or *E*-enolate.[3,10-13] The difference between dialkoxylboron enolates (borates), which give syn products from either *Z*- or *E*-enolates, and dialkylboron enolates (borinates), which follow the same stereochemical preferences as lithium enolates, is particularly striking. The nature of strong coordinating power of these metal ions with oxygen makes the "open" acyclic transition state less attractive than the cyclic transition state model.

Nakamura and Kuwajima proposed that a twist-boat transition state involving the *E*-enolate of titanium is more favorable than the corresponding chair transition state, whereas the *Z*-enolate undergoes the aldol reaction via the normal chair transition state.[10c] This boat/chair switching scheme (Figure 6) for *E*- and *Z*-enolates was also suggested for the aldol reaction involving enol borates.[11] Boat

transition structures for *E*-enolates are suggested to be involved whenever both *Z*- and *E*-enolates give syn products through cyclic chelated transition states. Hoffmann et al. proposed that a twist-boat transition structure occurs with *E*-enol borates.[12] MNDO calculations by Gennari et al. predict rather flat half-chair and twist-boat conformations for enol borinate (BR₂) and borate (B(OR)₂) aldol reactions.[13] The torsional angles are about 52–60° for the half-chair and 5–20° for the twist-boat in these model calculations, as compared to 60° and 0°, respectively, for idealized chair and boat structures.

Seebach and Golinski have proposed more generally that aldol reactions and related carbon–carbon bond-forming reactions of unsaturated molecules prefer the transition states shown in Figure 7. Here, D and A represent the unsaturated groups on donor- and acceptor-substituted molecules, such as an enolate and an aldehyde.[14] R_D, the substituent on the donor, prefers the conformation shown in (a), since when situated as in (b), there will be repulsion of R_D with R_A and H on acceptor molecule. This repulsion may arise as shown in (c), which is another view of (b). R_A will prefer to be situated anti to D.

Recently, Anh and Thanh proposed a different model 4 for the aldol transition state, shown in Figure 8. It has the enolate and carbonyl moieties in parallel planes and the carbonyl $C_1=O_2$ located right on top of the connecting line between C_3 and O_5. The torsional angle around the forming CC bond is about 30°. This structure is based
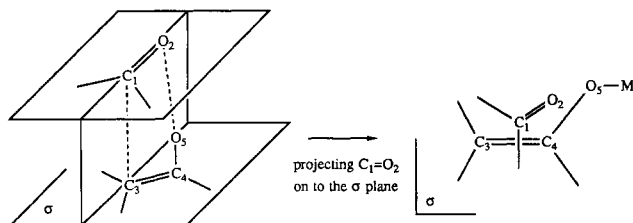
Figure 8. The Anh–Thanh transition state model (4) for aldol reactions.

upon model calculations on hydride attack on acetaldehyde, and considerations of frontier orbital interactions between enolates and aldehydes.[15]

It is clear that a great many models have been proposed, and they all help account for some data. They are not likely all to be correct! Our theoretical studies have been undertaken in order to determine which of these models are adequate representations of transition states and how metal cations, solvents, and substituents alter the transition-state geometries.

Computations

Reactants, complexes of the reactants, transition structures, and the preferred conformation of the products were located with the 3-21G basis set[28] and the GAUSSIAN 80 and 82 programs.[29] The Berny optimization program with gradient calculations was used to optimize structures that have acyclic geometries. Optimizations of cyclic structures with the Berny method can be difficult in some cases, and the Murtaugh–Sargent optimization algorithm was thus used. Alternatively, optimizations of cyclic structures can be carried out by reading in the force constants generated by the frequency calculations of a trial geometry with a smaller basis set (e.g. STO-2G). The starting trial geometry was located by optimizations with a smaller basis set. To locate a transition structure, we used the forming CC bond as the reaction coordinate. Optimizations were performed with several constrained CC bond lengths, and the geometry corresponding to the maximum energy was selected as a trial geometry for transition-structure optimization. From this geometry, the Berny optimization was used to optimize to a saddle point. For cyclic transition structures, it is important to first calculate the force constants of the initial trial geometry with a smaller basis set and read in these force constants for subsequent transition-structure optimization. Each stationary point was fully optimized[30] and characterized according to the number of positive and negative eigenvalues of the force constant (Hessian) matrix. Reactants, complexes, and products each have no negative eigenvalues, while transition structures have only one. Single-point energy evaluations were carried out with the 6-31G* or 6-31+G basis sets, which have d orbitals[31] or diffuse s and p functions,[32] respectively, on heavy atoms.

(28) Binkley, J. S.; Pople, J. A.; Hehre, W. J. *J. Am. Chem. Soc.* **1980**, *102*, 939.

(29) GAUSSIAN 80 and 82, Binkley, J. S.; Frisch, M.; Raghavachari, K.; DeFrees, D.; Schlegel, H. B.; Whiteside, R.; Fluder, E.; Seeger, R.; Pople, J. A.; Carnegie-Mellon University: Pittsburgh, PA. The DEC-10 and Harris 800 versions, converted by Dr. John Yates, were used for some of these calculations.

(30) Full geometries are available as supplementary material. The total energies of acetaldehyde enolate, formaldehyde, lithium acetaldehyde enolate, and boron acetaldehyde enolate are −155.42195, −113.22182, −158.92118, and −177.20935 au at the 3-21G level.

(31) The 6-31+G//3-21G gave similar relative energies to 6-31G*// 3-21G for these species, but the latter gave lower energies. The 6-31G* basis set: Hariharan, P. C.; Pople, J. A. *Chem. Phys. Lett.* **1972**, *16*, 217.

(32) Clark, T.; Chandrasekhar, J.; Spitznagel, G. W.; Schleyer, P. v. R. *J. Comput. Chem.* **1983**, *4*, 294.
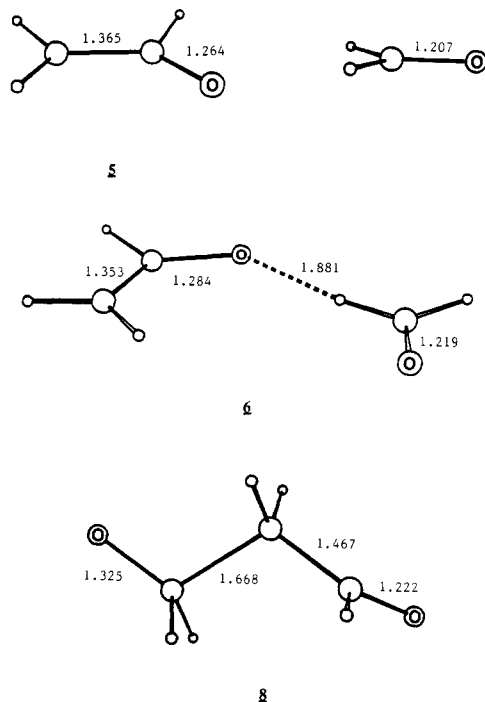

Figure 9. 3-21G optimized geometries of enolate anion (5), the ion–molecule complex (6), and the product (8) for the reaction of acetaldehyde enolate with formaldehyde.
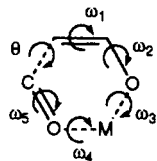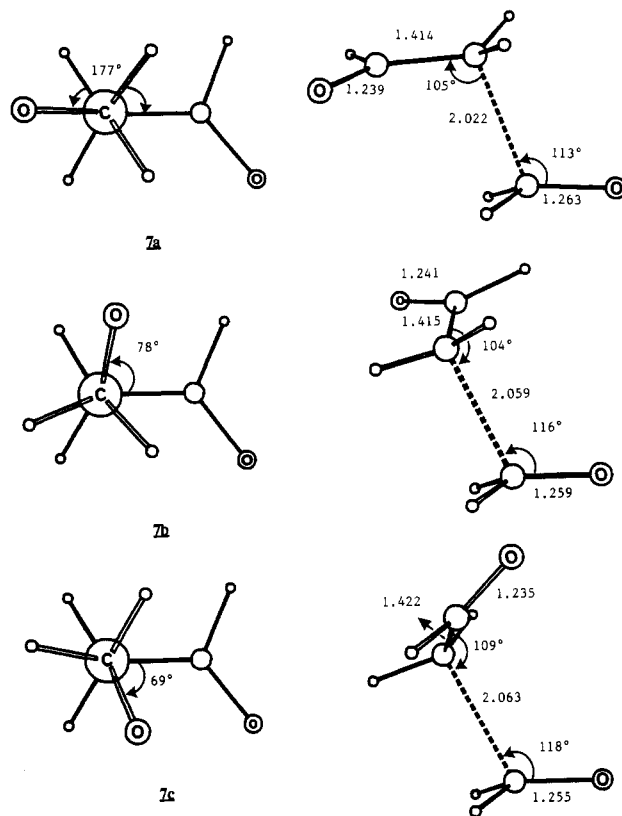

Figure 10. 3-21G optimized geometries of transition structures (7a–c) for the reaction of acetaldehyde enolate with formaldehyde.

Results and Discussion

Acetaldehyde Enolate plus Formaldehyde. The energetics of the reaction of acetaldehyde enolate with formaldehyde at the 3-21G level are given in Table II. Single-point calculations at the 6-31G* level[31] were also carried out on the reactants, three transition structures, and product, and the relative energies are shown in eq 2.

Table II. Calculated Reaction Energetics (kcal/mol) of Various Aldol Reactions and the Optimized Torsional Angles for the Complexes and Transition Structures

species	energies	angle, deg					
		θ	ω_1	ω_2	ω_3	ω_4	ω_5
$CH_2=CHO^- + CH_2=O$	0.0^a						
$[CH_2=CHO\cdots CH_2=O]^-$	-19.2						
transition structure 7a	-7.6	177	83				
transition structure 7b	-7.7	78	94				
transition structure 7c	-4.3	-69	99				
$O=CHCH_2CH_2O^-$	-9.7	173	101				
$CH_2=CHOLi + CH_2=O$	0.0^b						
$CH_2=CHOLi\cdots O=CH_2$	-28.0			4	129	-132	
transition structure 11	-26.0	-48	69	-52	-3	8	15
$O=CHCH_2CH_2OLi$	-40.2	-56	58	-23	-9	4	27
$O=CHCH_2CH_2OH^c$		-61	7	23			68
$trans\text{-}CH_2=CHOBH_2 + CH_2=O$	0.0^d						
$cis\text{-}CH_2=CHOBH_2 + CH_2=O$	0.7						
$trans\text{-}CH_2=CHOBH_2\cdots O=CH_2$	-6.4			179	-84	-171	
$cis\text{-}CH_2=CHOBH_2\cdots O=CH_2$	-10.2			23	-90	-14	
chair transition structure 18	1.8	-57	68	-84	54	-61	64
boat transition structure 19	0.4	-25	57	-25	-48	75	-37
$O=CHCH_2CH_2OBH_2$	-32.0	-63	-1	28	-15	-27	78

^{a} Total energy: -264.64377 au. ^{b} Total energy: -272.14300 au. ^{c} Total energy: -265.31219 au. ^{d} Total energy: -290.43117 au.

The optimized geometries, and their relevant geometrical parameters are shown in Figures 9 and 10. We begin by describing the energetics and then discuss the geometrical features of the transitions states.
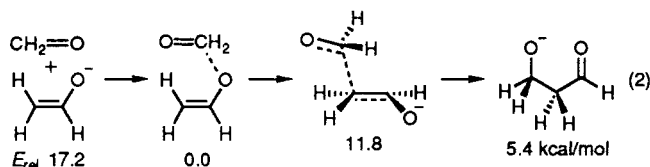
The experimental heat of the reaction of acetaldehyde enolate with formaldehyde can be estimated from the thermodynamic cycle shown in Figure 11. The heat of reaction of formaldehyde with acetaldehyde can be calculated from the heats of formation of reactants[33] and the estimated heat of formation of the aldol product from Benson's group equivalents.[34] In this way, ΔH is estimated to be -14.6 kcal/mol. The proton affinity of acetaldehyde enolate is 366.4 kcal/mol,[35] while that of aldolate can be estimated to be somewhat lower than the 374 + 3 kcal/mol PA of primary alcohols,[36] since aldolate should be stabilized to some extent by the β-keto group. Using a value of 370 kcal/mol, ΔH_{rxn} is calculated to be -11 kcal/mol, somewhat less exothermic than the reaction of the neutrals. Even if the β-carbonyl does not stabilize the primary alkoxide product, the reaction should be slightly exothermic. At the 3-21G level, the reaction is predicted to be exothermic by 10 kcal/mol, in reasonable agreement with the thermochemical estimate. The 6-31G*//3-21G calculations predict that the reaction is exothermic by 12 kcal/mol.
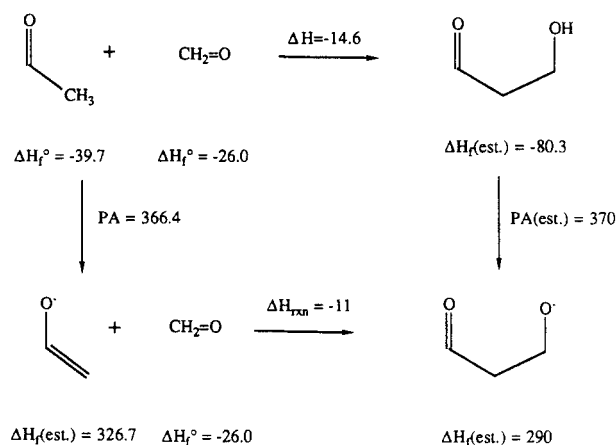

Figure 11. Estimated enthalpies (kcal/mol) of the aldol reaction of acetaldehyde with formaldehyde in the gas phase.

The ready reversibility of reactions of relatively "free" enolates in solution has been interpreted as evidence that the aldol reaction is endothermic and only becomes irreversible when a cation or other species traps the product aldolate.[3,8] Both thermochemical and theoretical estimates suggest that the reaction is somewhat exothermic starting from the isolated reactants in the gas phase, although it should readily reverse, which can account for equilibria between isomeric products.

The reaction is predicted to have a significantly negative activation energy in the gas phase. The ion–molecule complex (6) is relatively stable, and the barriers of reaction are 12–15 kcal/mol, starting from this complex. The calculated activation energy for the retro-aldol reaction to form the ion–molecule complex is only 2–5 kcal/mol. These calculations predict that the reaction of a simple enolate in the gas phase should produce the ion–molecule complex, which is more stable than the aldolate product (8). Bartmess has observed reactions of enolates with esters, but these reactions can proceed with loss of an

(33) Cox, J. D.; Pilcher, G. *Thermochemistry of Organic and Organometallic Compounds*; Academic Press: New York, 1970.

(34) Benson, S. W. *Thermochemical Kinetics*, 2nd ed.; Wiley-Interscience: New York, 1976.

(35) Bartmess, J. E. In *Gas Phase Ion Chemistry*; Bowers, M. T., Ed.; Academic Press: New York, 1979; Vol. 2, p 111.

(36) Bartmess, J. E. In *Gas Phase Ion Chemistry*; Bowers, M. T., Ed.; Academic Press: New York, 1979; Vol. 2, p 107.

alkoxide.[37] Another likely gas-phase reaction would be attack of the enolate oxygen on formaldehyde. This process is calculated to be exothermic by 23 kcal/mol and will not have any appreciable barrier, as was found for other alkoxide attacks on aldehydes.[23a,24,25]

Three distinct transition structures (7a–c) were located for the reaction of the metal-free acetaldehyde enolate with formaldehyde. In spite of the exothermicity of the reaction, the transition structures are nearly halfway between reactants and products in terms of bond lengths of the enolate and formaldehyde moieties. The reactions actually involve the conversion of the ion–molecule complex 6 into the product 8, a process which is endothermic by 9.5 kcal/mol. The forming CC bond lengths are 2.0–2.1 Å, a distance range which is common to other carbon–carbon bond-forming processes, such as the Diels–Alder reaction,[38] the Cope rearrangement,[39] the cycloaddition of fulminic acid to acetylene,[40] and the electrocyclization of butadiene.[41] The trajectory of attack of the nucleophilic enolate carbon on formaldehyde is 113–118° in the three different transition structures, consistent with our generalization that nucleophiles attack unsaturated bonds with an angle which is larger than tetrahedral,[26] whereas most other studies suggest a tetrahedral approach angle.[21,22] In spite of larger than tetrahedral attack angles, both carbons at the reaction center were pyramidalized, and there is no obvious steric repulsion of the type offered as a reason for the Seebach–Golinski rule for nonchelated transition structures.[14] Electrophilic attack on the enolate occurs with a somewhat smaller angle of 104–109°. For each transition structure, Mulliken population analyses indicate that there is 0.34–0.35 charge transfer from the enolate moiety to the aldehyde. Both oxygens have nearly the same amount of negative charge (−0.67 to −0.75) in the transition structures, indicative of 50% reaction progress.

Perhaps the most surprising conclusion of these calculations is the similar energies of the three transition structures. The three transition structures (7a–c) have θ = 177°, 78°, and −69°, and all are more or less staggered about the forming CC bond. At the 6-31G*//3-21G level, the relative energies of the 177°, 78°, and −69° transition structures are 0.0, 0.0, and 3.4 kcal/mol, respectively. We have estimated the energy required to alter θ in the following way. When a rigid rotation of the θ = −69° transition structure to θ = 0° is carried out, the 3-21G energy increases by 1.5 kcal/mol. Starting from the 78° transition structure, a rigid rotation to θ = 0° increases the energy by 5.4 kcal/mol. Although these calculations give only upper limits to the difference between staggered and eclipsed transition structures, they do suggest that there is significant preference for staggering even about the long, partially formed CC bond.[42]

Transition structures 7a and 7b are nearly equal in energy, while transition structure 7c (θ = −69°) is 2–3 kcal/mol higher in energy. The O–O distances in these three structures are 4.56, 4.24, and 3.8 Å, respectively, and

Enolate dianion

moderate threo selectivity   enhanced threo selectivity
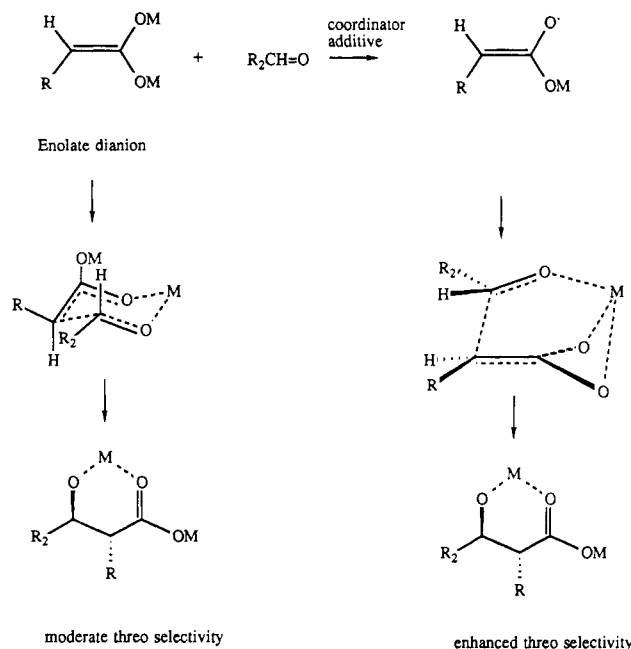
Figure 12. Transition-state models for the reaction of carboxylic acid dianions with aldehydes in the presence of strong cation coordinators.

presumably the transition structure 7c is highest in energy due to the electrostatic repulsion between the two partially negative oxygens.[43a] According to a Mulliken population analysis, the formaldehyde and enolate oxygens both have charges of about −0.7 in the transition structures. Since the two synclinal conformers are so close in energy to the anti, all these conformations should be considered in order to predict stereochemistries of this type of reaction. Recent experimental studies on metal-free enolate aldol reactions suggested that the synclinal transition-state model 7b would be more favorable than the anti 7a when the R₁ substituent of the enolate is small.[43b]

The product enolate (8) is appreciably distorted, consistent with the expected stabilization of the alkoxide by the carbonyl. While the carbonyl double bond is only slightly longer than that of a normal carbonyl group, the β-CC bond is stretched to 1.67 Å (cf. 1.54 Å for a normal CC bond). The CO bond of the alkoxide is contracted to 1.37 Å, versus 1.43 Å for a normal CO single bond. The distortions are those expected for a molecule preordained to undergo easy retro-aldol reaction. They may be exaggerated by the use of small basis set.

The transition structures have all bonds 40–50% distorted from reactants toward products. In the 177° and 78° transition structures, the carbonyl carbon attacks the enolate double bond in a plane perpendicular to the enolate plane. On the other hand, the C···C=C—O torsional angle is greater than 90° in the −69° transition structure 7c in order to relieve O–O repulsion. Since the repulsive electrostatic interactions are overwhelming in the −69° transition state as indicated by its unfavorable energy and distorted geometry, attractive secondary orbital interactions (if any) cannot be of significant importance to control the stereochemistry of metal-free aldol reactions. In the case of the reaction of the carboxylic acid dianion with aldehyde,[9] the increasing anti selectivity caused by the addition of cation coordinators may be due to a

(37) Bartmess, J. E.; Hays, R. L.; Caldwell, G. *J. Am. Chem. Soc.* **1981**, *103*, 1338.

(38) (a) Brown, F. K.; Houk, K. N. *Tetrahedron Lett.* **1984**, 4609 and references therein. (b) Houk, K. N.; Lin, Y.-T.; Brown, F. K. *J. Am. Chem. Soc.* **1986**, *108*, 554.

(39) Osamura, Y.; Kato, S.; Morokuma, K.; Feller, D.; Davidson, E. R.; Borden, W. T. *J. Am. Chem. Soc.* **1984**, *106*, 3362.

(40) Goddard, J. D.; Komornicki, A.; Schaefer, H. F. III *J. Am. Chem. Soc.* **1980**, *102*, 1763.

(41) Kirmse, W.; Rondan, N. G. Houk, K. N. *J. Am. Chem. Soc.* **1984**, *106*, 7989.

(42) The difference in energy between the staggered and eclipsed transition structures for attack of CH₃⁻ on ethylene (N.G. Rondan, unpublished results) is 0.2 kcal/mol.

(43) (a) Denmark, S. E.; Henke, B. R. *J. Am. Chem. Soc.* **1989**, *111*, 8032. (b) Nakamura, E.; Yamago, S.; Machii, D.; Kuwajima, I. *Tetrahedron Lett.* **1988**, 2207. We thank Professor Kuwajima for sending us the manuscript before publication.
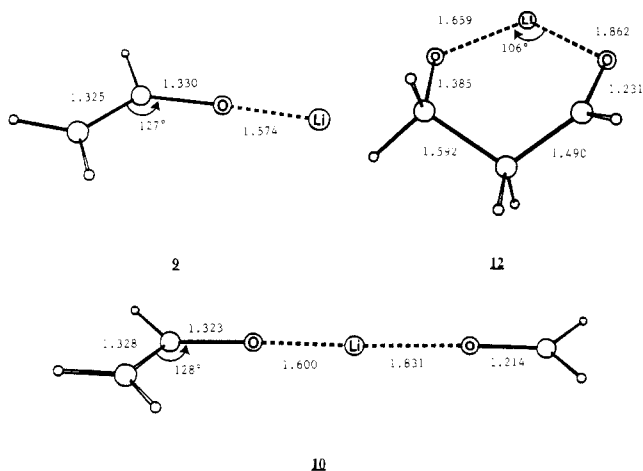
Figure 13. 3-21G optimized geometries of the lithium acet-aldehyde enolate (9), the lithium enolate complex (10), and the lithium aldolate (12) for the reaction of lithium acetaldehyde enolate with formaldehyde.

strengthening of the chelation in the transition state because better solvation of one of the two cations leaves only one to form a nicely bridged species as postulated in Figure 12.

Lithium Enolate plus Formaldehyde. The structure of lithium enolate has been investigated at various levels.[44] As shown in Figure 13, the 3-21G structure 9 compares favorably with these structures. The optimized lithium enolate resembles the enol structure more than the enolate anion (5). It is expected that solvation of lithium cation would give a more enolate-like structure.

The calculated energetics for the reaction of lithium enolate with formaldehyde are shown in Table II. Since these calculations are for the gas-phase unsolvated species, there is a large (28 kcal/mol) stabilization upon coordination of the lithium of the enolate with formaldehyde. In solution, in coordinating solvents, or when the lithium enolate is aggregated, the coordination with the carbonyl is expected to be less exothermic, or perhaps approximately thermoneutral as compared to coordination of lithium with an oxygen of an ether solvent molecule. The geometry of the complex (10) may also differ in solution, since the lithium should assume more or less tetrahedral coordination, bringing the enolate and carbonyl moieties closer. The calculated activation energy beginning from the complex is extremely low, only 2 kcal/mol, most of which is probably due to twisting the reactants with respect to lithium into a less favorable coordination arrangement. From the complex 10 to the product 12, the reaction is calculated to be exothermic by 12 kcal/mol at the 3-21G level.

There is only one lithium enolate transition state (11), and it is shown in Figure 14. It is a half-chair, with the Li+ approximately in the plane of the adjacent four atoms. Since the Li–O interactions are mainly electrostatic in nature, this general shape could also be present in the aggregates involved in reactions in solution.[45] Indeed, this geometric feature is consistent with geometries determined by X-ray crystallographic studies of tetrameric enolate complexes and a tetrameric aldolate product, in which the bridging Li+ and the adjacent four atoms are also in the same plane.[46]
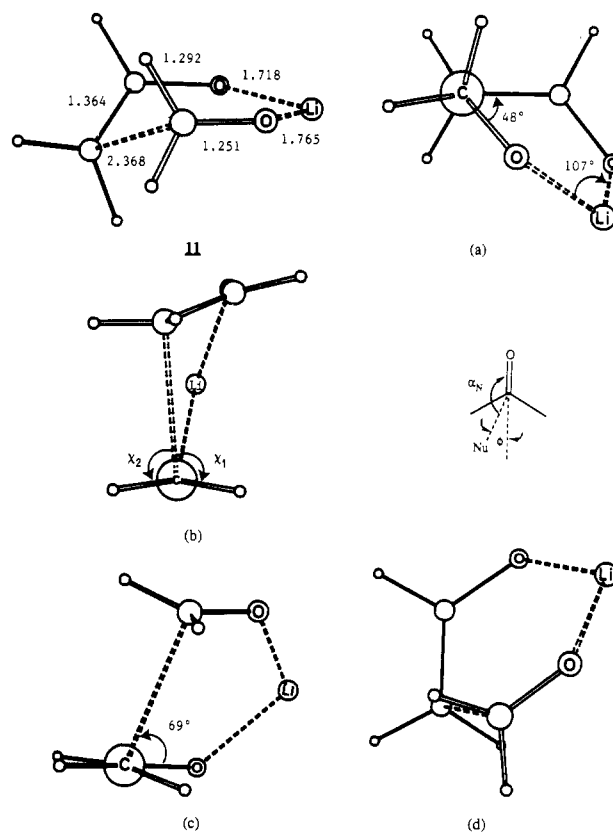

Figure 14. Views of the 3-21G transition structure (11) of the aldol reaction of lithium acetaldehyde enolate with formaldehyde.

In spite of the low activation energies, there is appreciable (20–30%) bond making and breaking in the transition structure (11) with respect to the conversion of complex (10) into product (12). Whatever the exact effect of solvation, it is certain that the reaction in solution will be much less exothermic than calculated for this gas-phase reaction of the lithium enolate, so that the transition structure of a solution reaction should be later than that calculated here. In spite of these cautions, the calculated transition structure does reveal interesting features resulting from coordination as compared to the reaction of the free anion, described earlier in this paper. In particular, the C=C···C=O torsional angle θ is reduced from −69° for the free enolate to −48° for the lithium enolate in order to facilitate coordination of lithium, which places the hydrogens (or substituents in substituted cases) in a relationship shown most clearly by the Newman projection in Figure 14 (view a).

The attack angle of the nucleophilic enolate on formaldehyde is 107°, whereas the attack angle on the enolate is 93°. Both nucleophilic and electrophilic attack angles are smaller than the corresponding angles for the reaction of the enolate anion with formaldehyde. Intramolecular coordination of lithium cation with oxygens causes a displacement of the nucleophilic attack trajectory from the plane which bisects the pyramidalized formaldehyde moiety. Therefore, three-dimensional terms are required to describe the trajectories of aldol reactions of both symmetrical and asymmetrical aldehydes and ketones. Liotta et al.[25a] used the angle of attack and an additional parameter ϕ to define the trajectories of nucleophilic attack at unsymmetrical carbonyl groups. However, the ϕ trajectory is difficult to define properly due to the pyrami-

(44) Lynch, T. J.; Newcomb, M.; Bergbreiter, D. E.; Hall, M. B. *J. Org. Chem.* **1980**, *45*, 5005.
(45) For a review of crystal structures of enolates: Seebach, D. *Angew. Chem., Int. Ed. Engl.* **1988**, *27*, 1624 and references therein.

(46) (a) Williard, P. G.; Salvino, J. M. *Tetrahedron Lett.* **1985**, 3931. (b) Williard, P. G.; Carpenter, G. B. *J. Am. Chem. Soc.* **1986**, *108*, 462.
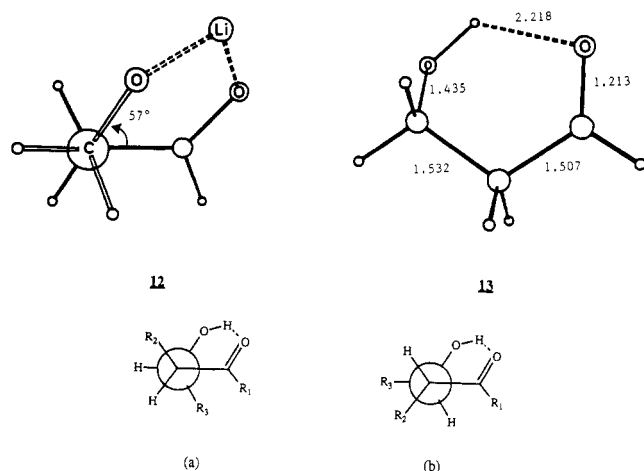
Figure 15. The 3-21G geometry of aldol product (13) and the preferred conformations of aldol products.

dalization of the carbonyl carbon in the transition state. We use the alternative parameters χ_1 and χ_2, which are the torsional angles of the Nu—C=O—H(axial) and Nu—C=O—H(equatorial), respectively. Angle χ_1 and χ_2 of the transition structure 11 were calculated to be 104° and 94°, as shown in Figure 14 (view b).

Figure 14 (view c) shows the Newman projection along the enolate CC bond. This indicates that the C···C=C—O torsional angle is also constricted from ~90° in the free enolate anion transition structure to 69° in the lithium coordinated case. If the carbonyl moiety is projected onto the enolate plane as shown in Figure 14 (view d), we can see that the carbonyl carbon is right above the cis-H of the enolate in contrast to the model proposed by Anh et al.[15] This deviation from perpendicular attack and the rigidity of the enolate π system produce an unequal amount of bending of the terminal enolate hydrogens. The hydrogen cis to the enolate oxygen is bent out of plane more significantly than the trans-hydrogen (view c), and a steric bulky group at the cis position is expected to push the carbonyl moiety to the stereoelectronically more favorable trajectory, namely, the perpendicular attack. Since the aldehyde attacks the enolate double bond from the side of the enolate oxygen, remote from the R_1 group, low stereoselectivities are predicted for unsubstituted enolates (with chiral R_1*)[2d] and E-enolates. On the other hand, Z-enolates have the incoming aldehyde closer to the R_1 group in the transition structure due to the steric repulsion of R_Z with the aldehyde moiety, and relative high selectivity can be accounted for.

The feature of coplanarity of the Li^+ and the adjacent four atoms of the transition structure is maintained in the product (12), which has a particularly long newly formed CC bond α to the alkoxide. The newly formed CC bond in the lithium aldolate is intermediate between the corresponding CC bond in the aldolate anion (8) and that of the aldol product (13). The calculated torsional angle θ in the product is -56° as compared to -72° in the crystal structure of tetrameric adduct of lithium pinacolonate with pivaldehyde.[46a] The structure of the lithium aldolate product, shown in a side view in Figure 15, is helpful in rationalizing the greater thermodynamic stability of threo (anti) aldolate products than erythro.[3] Both lithium aldolate and aldol product adopt the most stable staggered conformation around the formed CC bond. Since the oxygens are bound in a gauche conformation as the result of lithium coordination or hydrogen bonding, the alkyl group R_3 would be either anti to the R_2 (a) or to the carbonyl functional group (b) in order to avoid steric inter-

actions between these groups. In any case, the threo or anti product is more stable than the erythro or syn product.

Methyl Effects. The effect of alkyl substituents on the stereochemistry of aldol reaction was evaluated qualitatively by replacing the hydrogens by a standard methyl group at various positions in the transition structure (11) and carrying out single-point calculations with the 3-21G basis set. For the reaction of lithium acetaldehyde enolate (R_1 = H) with acetaldehyde, the preference of the quasi-equatorial over the quasi-axial position is small for the methyl group at the carbonyl carbon of the acetaldehyde moiety. The preference increases by 1.6 kcal/mol when R_1 is changed from hydrogen to a methyl group (i.e. ketone enolate).

Solvated Models. A more realistic energetic situation is approximated by the calculations carried out with three solvent molecules. Three standard waters were used to model ether solvent. The lithium cation of lithium enolate is tetrahedrally coordinated by the three oxygens of water molecules with OLi bond lengths of 2.0 Å. The energy of the solvated complex was estimated by placing two water molecules on lithium and carrying out partial optimization of the bond angles around lithium. The energy of the solvated transition structure and product was approximated by adding two waters in a similar way to the transition structure and the product as shown below:
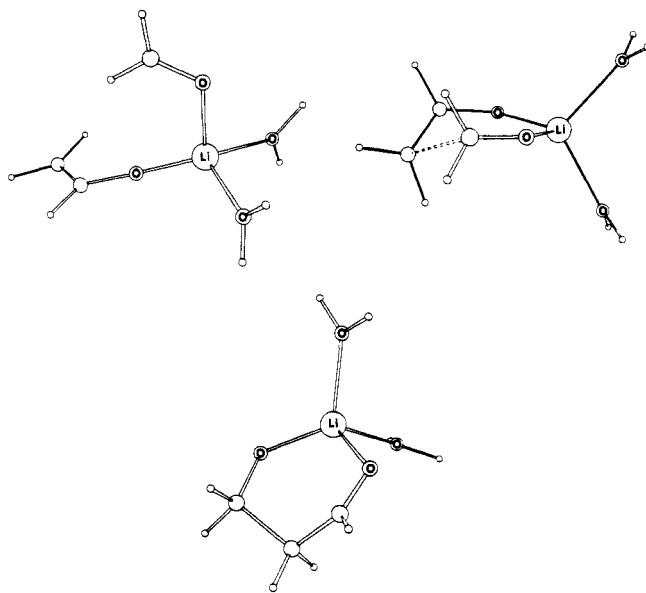
For the energetic comparison, the energy of a single isolated water molecule was included in the calculation of the latter three species. In this way, the relative energies of solvated reactants, complex, transition structure, and product in solution are crudely estimated to be 0.0, -4.5, -4.2, and -17.1 kcal/mol, respectively. The calculated heat of reaction is in good accord with recent measurement of the heat of reaction for the reaction of lithiopinacolonate with pivalaldehyde in hexane/THF solution.[47]

The 3-21G transition structure of the reaction of lithium enolate with formaldehyde has relative short lithium-oxygen distances (1.7–1.8 Å) as compared to those observed in crystal structures of tetrameric complexes and aldolate (1.9–2.1 Å). The interactions between solvated lithium cation and oxygens are expected to be considerably weaker than those in the gas phase, and a longer lithium oxygen

(47) Arnett, E. M.; Fisher, F. J.; Nichols, M. A.; Ribeiro, A. A. *J. Am. Chem. Soc.* **1989,** *111,* 748.
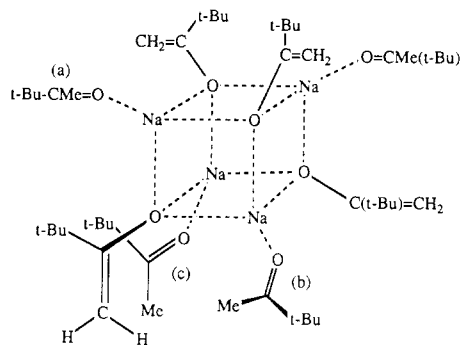
Figure 16. The structure of sodium enolate complex with ketone as revealed by X-ray crystallography.

separation may cause an increase of the torsional angle, θ, of the transition state in solution. In order to understand the relationship between the torsional angle θ and the lithium–oxygen distance, we carried out calculations based on a rigid rotation of lithium enolate transition structure around the forming CC bond. At the rotational angles of $\theta = -48°$, 60°, and −90°, the O⋯O distances are 2.8, 3.5, and 3.3 Å, respectively. Optimization of lithium position in these rigid conformations indicates the lithium–oxygen distances fall into the range of 1.9–2.0 Å with the O–Li–O angle around 120°. It seems that both synclinal and skewed 90° transition structures are possible for the given lithium–oxygen distance in solution. However, calculations with constraints of lithium–oxygen distances (2.0 Å) and the forming CC bond (2.36 Å) predict the torsional angle θ to be around −60°, which indicates that a −90° torsional angle is not essential to accommodate the 1.9–2.1 Å metal–oxygen distances in solution.

Recent X-ray crystallographic characterization[46b] of tetrameric sodium pinacolonate solvated by pinacolone provides some interesting information about how the preformed ketone–enolate complex undergoes the aldol reaction. As shown in Figure 16, the enolate adopts a preferred conformation with the C=C double bond *anti* to one of the adjacent O—Na bonds, as is commonly observed also in other tetrameric enolate structures.[45] For each enolate moiety, there are three neighboring solvated ketones available to react with, but only one of them is in a conformationally favorable arrangement. Ketone (a) which is coordinated with the sodium anti to the enolate double is unlikely to react with that enolate. Ketone (b) has the alkyl group pointing toward the nearby enolate plane and is not in position to react. On the other hand, the conformationally well-oriented ketone (c) has its π-system facing the π-system of the enolate with 3.85-Å separation between the reacting carbon centers. The *tert*-butyl group of the ketone is on the same side of the bulky *tert*-butyl group of the enolate, which corresponds to the conformation of the pericyclic transition state that gives the minor aldol product. Presumably, only this less reactive enolate complex could be isolated and characterized, whereas the aldol reaction would readily occur if the *tert*-butyl group of the ketone took the quasi-equatorial position, away from the *tert*-butyl group on the enolate moiety. The O=C⋯C—C torsional angle in the crystal structure of the complex is 67°, and the attack angle on the ketone double bond is 73°. This small attack angle is expected to become larger than 90° in the transition state, and the electrophilic attack angle on the enolate should decrease from 108° revealed by X-ray to some extent.

Boron Enolate plus Formaldehyde. The transition structures for the reaction of the parent boron enolate with
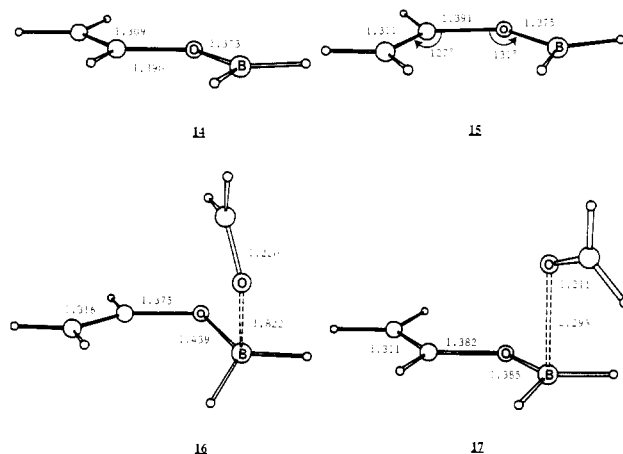

Figure 17. 3-21G geometries of the s-cis and s-trans enol borinates and complexes of enol borinates for the reaction of enol borinate of acetaldehyde with formaldehyde.
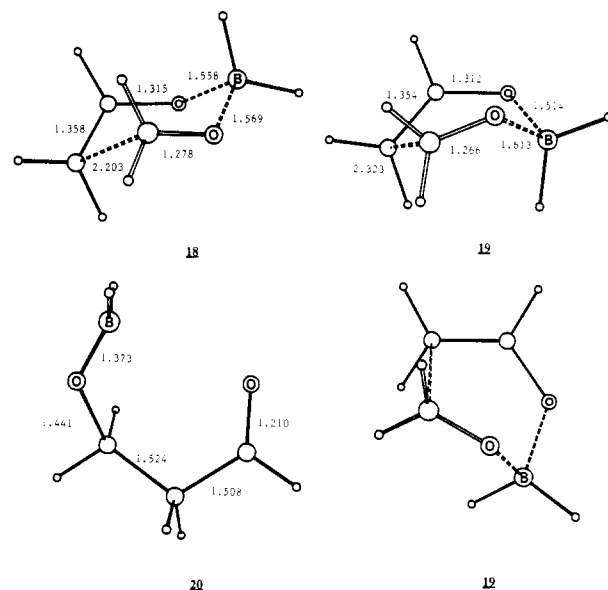

Figure 18. 3-21G geometries of the chair (18) and twist-boat (19) transition structures and the boron aldolate (20) for the reaction of enol borinate of acetaldehyde with formaldehyde.

formaldehyde were located by the same procedure as before. The energetic profile of the reaction is shown in Table II. Figure 17 shows the optimized reactants, complexes, and product. The chair and twist-boat transition structures are shown in Figure 18.

The preferred structure of the free boron enolate has an s-trans conformation (14, torsional angle CCOB = 180°), with a 2 kcal/mol rotational barrier. The 3-21G calculations indicate that the s-trans conformation of the parent enol borinate is 0.7 kcal/mol more stable than the s-cis conformation (15). The 3-21G calculations predict that the s-trans conformation is also preferred for both *E*- and *Z*-enolates of propionaldehyde, while the alkyl substituent at the α-position of the enolate disfavors the s-trans conformation.[48] MNDO and STO-3G calculations predict that the ground-state conformations of both enol borinate and enol borate are s-cis for the *E*-enolate and s-trans for the *Z*-enolate.[12]

In the gas phase, the reaction mechanism involves formation of a Lewis acid–base adduct between the metal

(48) Goodman, J. M.; Paterson, I.; Kahn, S. D. *Tetrahedron Lett.* **1987**, 5209. We thank Professor Kahn for sending us the manuscript before publication.

Table III. Relative Energies and Geometrical Features of Transition Structures of Methyl-Substituted Aldol Reactions

TS[a]	E_R, kcal/mol	R_{C-C}, Å	angle, deg					
			α_E	α_N	θ	ω_1	χ_1	χ_2
21a (twist-boat, ax)	0.0	2.234	94	103	−26	57	115	92
21b (twist-boat, eq)	+1.6	2.283	93	101	−30	57	101	106
22a (chair, ax)	+4.2[b]	2.180	89	102	−55	67	117	95
22b (chair, eq)	+2.4	2.146	90	102	−57	66	107	104
23a (twist-boat)	0.0	2.400	90	102	−25	58	107	89
23b (chair TS)	+0.4	2.308	86	101	−59	67	102	97
24a (twist-boat)	0.0	2.332	90	104	−23	58	106	92
24b (chair TS)	+0.1	2.222	86	103	−57	67	106	97
25a ($Z \rightarrow$ twist-boat)	+4.0	2.316	85	108	−21	66	110	91
25b ($Z \rightarrow$ chair TS)	0.0	2.225	82	104	−59	74	109	96
26a ($E \rightarrow$ twist-boat)	0.0	2.330	89	105	−27	59	108	91
26b ($E \rightarrow$ chair TS)	+0.1	2.213	84	105	−56	70	107	97

[a] TS = transition state. [b] This is not an authentic transition structure; it collapses to the axial twist-boat upon optimization.

center and the carbonyl oxygen. The geometries of complexes of s-cis and s-trans enol borinates with formaldehyde are shown in Figure 17. In contrast to the isolated enol borinate, the complex with the enol borinate moiety of s-cis orientation (**16**) is 3.8 kcal/mol lower in energy than the s-trans complex (**17**). The O–B bond is longer for the s-trans complex than for the s-cis complex, which may account for the energy difference between them. From the s-cis complex to the product **20**, the reaction is exothermic by 22 kcal/mol with a 12 kcal/mol reaction barrier.

For the simplest enol reaction, both chair (**18**) and twist-boat (**19**) transition states were found. The calculated C=C···C=O torsional angles θ are −56° and −25°, respectively, in the chair and twist-boat transition structures. The twist-boat geometry is intermediate between the "Evans boat" and another feasible boat formed from **2** by moving the metal bowsprit. The twist-boat is lower in energy than the chair conformation by 1.4 kcal/mol. In the chair and the twist-boat transition structures, the C=C—O—B torsional angles are 84° and 25°, respectively. This twist-boat is preferred because the C=C—O—B torsional angle is closer to the ideal 0°,[12,13] and this structure also reduces the repulsion between the lone pairs on the two oxygens. In addition, the absence of hydrogens on enolate oxygen reduces the steric interaction in the boatlike transition state. These interactions were found to be significant in the boatlike transition state of allylborane addition to formaldehyde.[49]

The forming CC bond lengths in the chair and twist-boat transition structures are calculated to be 2.3 and 2.2 Å, respectively, which are shorter than that in the lithium enolate transition structure but are longer than those predicted for the transition structures involving the free enolate anion. The angles of attack in both chair and twist-boat transition structures are similar to those in the lithium enolate transition structure. Angle χ_1 is 106° for the chair and 108° for the twist-boat, while angle χ_2 is 98° for the chair and 91° for the twist-boat.

The small difference between the relative energies of the chair and twist-boat transitions structures prompted us to undertake systematic studies of the substituent effects on the chair and twist-boat transition structures. Transition structures were located for 12 methyl-substituted cases, as shown in Table III. The chair and twist-boat transition structures were located for the reaction of enol borinate with acetaldehyde, and are shown in Figure 19. The twist-boat conformations **21** are still preferred over
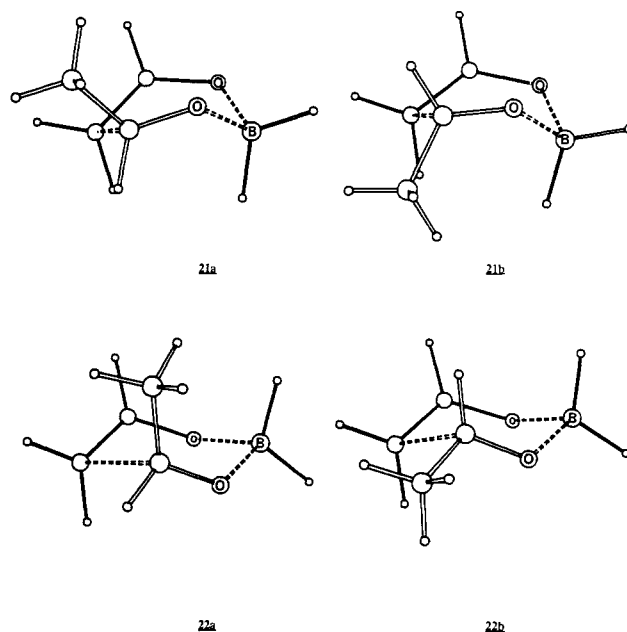

Figure 19. 3-21G transition structures for the reactions of enol borinate of acetaldehyde with acetaldehyde.

the chair transition structure **22** regardless of the position of the methyl group. Since the terms "axial" and "equatorial" are poorly defined for twist-boat conformation, we used axial or equatorial in the same sense as defined in the chair conformation. The methyl group prefers the quasi-equatorial position in the chair transition structure, whereas quasi-axial position is more favorable for the methyl group in the twist-boat transition structure.

Transition structures of the aldol reaction with acetaldehyde also provide quantitative information about how the trajectory of attack on the carbonyl group changes when the carbonyl group is unsymmetrically substituted. The angle χ_1 and χ_2 for axial and equatorial substituents at the carbonyl carbon, which are defined in a similar way as in the transition structure **11**, are also shown in Table III.

The α-alkyl substituent, R_1, influences the relative energies of the chair and boat to some extent. When the steric bulk of R_1 group increases from hydrogen to methyl, the preference for the twist-boat transition state (**23a**) over the chair (**23b**) decreases by 1 kcal/mol. Substituents on the boron may also switch the preference for either the chair or the boat. Replacement of the hydrogens on B by alkyl groups should destabilize the twist-boat, because the axial group on boron has 1,3- and 1,4-interactions with R_Z

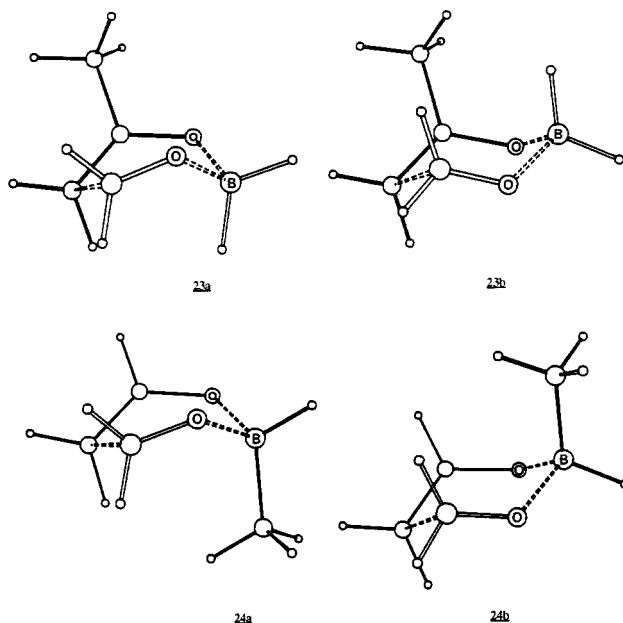(49) Li, Y.; Houk, K. N. *J. Am. Chem. Soc.* **1989**, *111*, 1236.

Figure 20. 3-21G transition structures for the reactions of the ketone borinate with formaldehyde and methylboron enolate with formaldehyde.

Figure 21. 3-21G transition structures for the reactions of *E*- and *Z*-enol borinates with formaldehyde.

and the group on the carbonyl carbon. Indeed, when the axial BH in the chair and twist-boat transition structures was replaced by a methyl, and calculation of the new transition structures were performed, the chair and the twist-boat transition structures (**24a–b**) are of the same energy. These transition structures are shown in Figure 20. Larger substituents on the boron should favor the chair even more. These calculations are in good agreement with the experimental observations that *Z*-enolates are much more stereoselective than the *E*-enolates, bulky R_1 improves the selectivity to some extent, and larger alkyl groups on boron moderately enhance the stereoselectivity.[3,5]

As shown in the Table III, the relative energies of chair and boat transition structures can be altered by substituents. *Z*-Enol borinates with large alkyl substituents strongly prefer the chair transition structure, because of strong destabilizing interactions between the bulky R_Z and groups on boron in the twist-boat transition structure. On the other hand, this destabilization is relative small when R_Z is hydrogen so that *E*-enolates prefer the chair less. Consequently, the *E*-enolates give lower stereoselectivity, because the minor products can be formed through twist-boat transition structures of comparable energies.

The geometric features revealed by these calculations support our rationalizations for different stereoselectivities of the *E* and *Z* lithium enolate reactions. As shown in Figure 21, the C···C=C—O torsional angles in transition structures of *E*- and *Z*-enolates are larger than that in the parent reaction, and the transition structure of the *Z*-enolate has the largest angle due to the steric repulsion imposed by the cis-methyl group. Consequently, the transition structure has the shortest distance between the α-hydrogen of the enolate and the axial hydrogen on aldehyde, in spite of the longest CC-forming bond. Therefore, relatively high selectivity is expected for the *Z*-enolate.

We have also located the chair and twist-boat transition structures for the reaction of acetaldehyde enol borate as shown in Figure 22. The chair transition structure **27** closely resembles the corresponding chair borinate, **18**. The chair transition structure **27** is 2.5 kcal/mol higher in energy than the twist-boat transition structure **28**. Since the alkyl substituent of the *E*-enolate is in a quasi-equa-
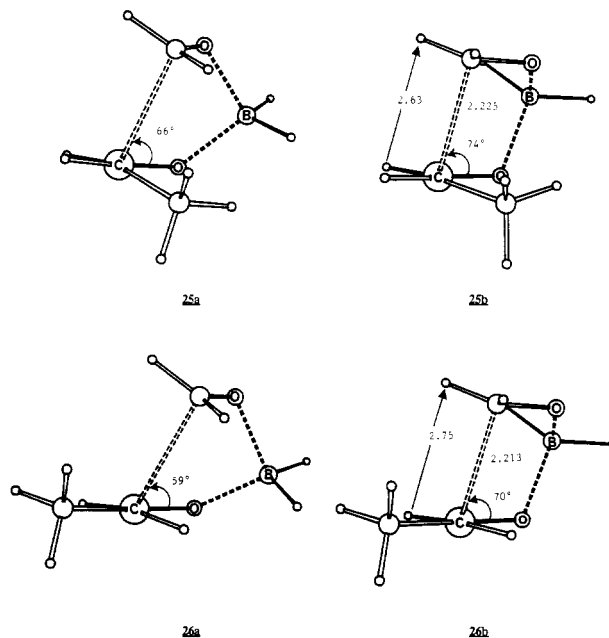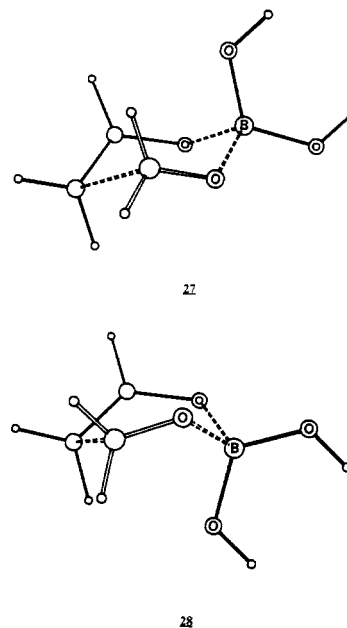

Figure 22. 3-21G transition structures for the reactions of enol borates with formaldehyde.

torial position in both chair and twist-boat transition structures, the relative energies of the chair and twist-boat transition are expected to be unchanged. The *E*-enolate will still prefer the twist-boat, and the preferred product will be the syn aldol. This is formed from the twist-boat transition structure with the aldehyde alkyl group almost eclipsed with the R_E group, which corresponds to a relatively unfavorable Evans boat. On the other hand, the 2.5 kcal/mol preference predicted for the twist-boat **27** will be overcome by the 4.0 kcal/mol preference for the chair which was predicted for the *Z*-enolate. For the reactions of *Z*-enolates, the preferred syn products will be formed from the chair transition structure with the alkyl group of the aldehyde adopting the equatorial position. Our theoretical results predict that is the origin of the preference for *Z*-enolates to react via the chair transition structure and give the syn product, and for *E*-enolates to react via the twist-boat transition structure and give the

syn product.[12] The larger preference for the twist-boat transition structure by the borate is related to the small size of the alkoxy substituent as compared with the alkyl substituent. In addition, the enol borate shows greater preference for planarity than the enol borinate. This is reflected by the 3.0 kcal/mol required to rotate the borate from planar to a 90° conformation at the 3-21G level, while the borinate requires only 2.0 kcal/mol. This conclusion is probably applicable to other stereoselective aldol reactions involving metal enolates, such as titanium and zirconium enolates, where the chair transition structure is favored for *Z*-enolates, but the twist-boat is favored for *E*-enolates.

Conclusion

There is a remarkable similarity of the forming CC distance in all the aldol reactions that we have studied. Dunitz–Bürgi attack angles of 101–108° are observed in both Li and BH_2 reactions.[21] The staggered conformations around the forming CC bond are also more stable than the corresponding eclipsed in spite of the long partially formed CC bond. Since both atoms forming the new bond are pyramidalized,[20a] there is no special crowding for the alkyl substituents on the reacting carbon centers in the nonchelated transition structures.

Cyclic transition structures were found for the aldol reactions involving lithium and boron enolates. The attack of carbonyl carbon on the enolate double bond deviates from the stereoelectronically preferred trajectory due to the coordination of the metal cation with oxygens in the cyclic transition structure. Secondary orbital interactions are of minor importance in controlling the geometrical features of the transition structure. For the parent reaction of boron enolate with formaldehyde, the twist-boat transition structure is 1.4 kcal/mol lower in energy than the chair. For the substituted cases, the chairlike transition structures are preferred for *Z*-enolates, while twist-boats are preferred for *E*-enolates.

Metal Ion Effects in Wittig Reactions: A General Hypothesis for the Mechanism of the Wittig Reaction

William J. Ward, Jr., and William E. McEwen*

*Department of Chemistry, University of Massachusetts, Amherst, Massachusetts 01003*

Received November 7, 1988

To evaluate better the effects of N_{2p}–P(IV) through-space interactions in Wittig reactions, a thorough study of metal ion effects in Wittig reactions lacking such interactions has been completed. As in the case of Wittig reactions with stabilized ylides, it has been determined that, with a moderated ylide, the stereochemistry (*E:Z* ratio) of alkene formation with an aldehyde is determined at the point that a new carbon–carbon bond has been formed to give a betaine or an oxaphosphetane intermediate. The observations that in most cases where lithium ion is present, the product mixture is enriched with the *Z* alkene, while when sodium or potassium ions are present, the *E* isomer predominates, are deemed to support the concept that a spin-paired diradical is formed as an unstable intermediate when sodium or potassium ions are present but that an ionic reaction occurs when lithium ions are present. The evidence that has been accumulated suggests that the reactions studied here (involving aromatic, heterocyclic, and aliphatic aldehydes and benzylidenediphenylmethylphosphorane or the preformed betaines, in THF at –78 °C) occur under kinetic control and without any significant degree of equilibration or Wittig reversal.

In an attempt to explore further the intricacies of the Wittig reaction, we embarked upon a detailed study of the reactions between a semistable ylide and a variety of aldehydes in the presence of lithium, sodium, or potassium ions.[1]

Results

Benzyldiphenylmethylphosphonium chloride, **1**, was converted to the ylide, benzylidenediphenylmethylphosphorane, **2**, by the action of an appropriate base, under

1   **2**
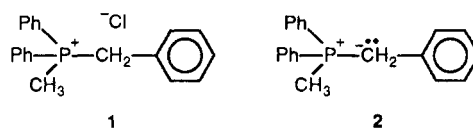
anhydrous conditions and an inert atmosphere. The solvent used throughout this study was anhydrous THF. The bases used to form the ylide were *n*-butyllithium, sodium dimsyl, sodium hexamethyldisilylamide (NaHMDS), or KHMDS. The red–orange ylide solution was then cooled and caused to react with a series of aromatic aldehydes, which are displayed in the data tables. An aliphatic aldehyde, pivalaldehyde, was also employed as a comparison with the reactions involving the aromatic

(1) This work was presented at the Fifth International Symposium on Inorganic Ring Systems (IRIS V), University of Massachusetts, Amherst, MA, Aug 8–12, 1988; *Phosphorus Sulfur Silicon* **1989**, *41*, 393.